Communication

A New Tailored Nano-Droplet Carrier of Astaxanthin Can Improve Its Pharmacokinetic Profile and Antioxidant Efficacy

Kumudesh Mishra , Nadin Khatib , Dinorah Barasch , Sharon Garti , Nissim Garti * , Or Kakhlon *

Posted Date: 9 April 2024

doi: 10.20944/preprints202404.0556.v1

Keywords: astaxanthin; nanodroplet formulations; oxidative damage

Communication

A New Tailored Nano-Droplet Carrier of Astaxanthin Can Improve Its Pharmacokinetic Profile and Antioxidant Efficacy

Kumudesh Mishra [1], Nadin Khatib [2], Dinorah Barasch [3], Sharon Garti [2], Nissim Garti [2,*] and Or Kakhlon [1,4,*]

[1] Department of Neurology, The Agnes Ginges Center for Human Neurogenetics,Hadassah-Hebrew University Medical Center, Jerusalem 9112001, Israel; kumudeshmishra@gmail.com
[2] Lyotropic Delivery Systems Ltd., Hi-Tech Park, Row 5(1), Edmond J. Safra Campus, Jerusalem 9139002, Israel; nadin@LDS-Biotech.com (NK), sharon@LDS-Biotech.com (SG)
[3] Mass Spectrometry Unit, Institute for Drug Research, School of Pharmacy, Hebrew University of Jerusalem, Jerusalem 9112102, Israel
[4] Faculty of Medicine, Hebrew University of Jerusalem, Jerusalem 9112001, Israel
* Correspondence: nissim@LDS-Biotech.com (NG), ork@hadassah.org.il (OK)

Abstract: Astaxanthin (ATX) is a carotenoid nutraceutical with a poor bioavailability due to its high lipophilicity. We tested a new tailored nano-droplet capable of solubilizing ATX in an oil-in-water micro-environment (LDS-ATX, manufactured by Lyotropic Delivery Systems (LDS)), for its capacity to improve ATX pharmacokinetic profile and anti-oxidant efficacy. We used liquid chromatography tandem mass spectrometry (LC-MS/MS) to compare the pharmacokinetic profile of ATX and LDS-ATX and protein carbonylation and lipid peroxidation assays to compare their basal and lipopolysaccharide (LPS)-induced oxidative damage. Our results show that only LPS-induced oxidative damage was corrected by ATX and LDS-ATX. While in the liver and muscle LDS-ATX was more efficacious than ATX in attenuating oxidative damage to both proteins and lipids, only oxidative damage to lipids was preferably corrected by LDS-ATX in the brain. These results strongly suggest improvement of ATX bioavailability and efficacy by the LDS-ATX nano-formulation.

Keywords: astaxanthin; nanodroplet formulations; oxidative damage

1. Introduction

Astaxanthin (ATX, β-Carotene-4,4'-dione, Trans-Astaxanthin), a xanthophyll carotenoid, is a red dietary carotenoid nutraceutical isolated from *Haematococcus pluvialis*. ATX is an antioxidant and anti-inflammatory FDA-approved supplement. Various reports (e.g., [1,2]) demonstrate ATX's safety and efficacy in counteracting aging-related disorders, diabetes, neurodegenerative disorders, cardiovascular diseases, immunodeficiency, Chagas disease, and more. All these beneficial effects are attributed to the relatively strong antioxidant capacity of ATX. However, the natural form of ATX is poorly bioavailable as an orally delivered substance [3] and as a result it requires a specific delivery system. We believe that the potency of ATX can be significantly improved by increasing its bioavailability through the use of tailored nanodroplets, already shown to improve the efficacy of other substances (*e.g.*, [4,5]). The aim of this study was therefore to test whether a tailored nanodroplet formulation of ATX (LDS-ATX), designed and manufactured by Lyotropic Delivery Systems (LDS) Ltd., is capable of improving the antioxidant capacity of ATX *in vivo* as manifested by protection against lipopolysaccharide (LPS)-induced oxidative injury. To that end, we used wild type mice in which oxidative injury was induced by LPS and assessed by protein carbonylation and lipid peroxidation assays on isolated tissues. Our results demonstrate the LDS-ATX is superior to oleoresin-dispersed ATX (AXT) in both improving bioavailability, and reducing LPS-induced oxidative damage to both protein and lipid in murine brain, liver, and muscle tissues.

 doi:10.20944/preprints202404.0556.v1

2. Results

2.1. Pharmacokinetics of LDS-ATX v ATX

To determine serum concentrations of ATX, plasmas from untreated mice was spiked with different concentrations of ATX. The standard curve thus generated (Figure 1) was used to interpolate ATX concentrations in the plasma. Our results (Figure 2) demonstrate that solubilizing ATX into the tailored nano-droplet formulation LDS-ATX leads to a significant accumulation of the drug in plasma over time. In addition, the halflife (t_{max}) of ATX in the plasma was delayed from 30 min in oleoresin ATX to 60 min in LDS-ATX. These two results strongly suggest that the bioavailability of ATX is significantly increased by its tailored nanodroplet formulation LDS-ATX compared to its classical commercially available product dispersed in oleoresin (AXT).

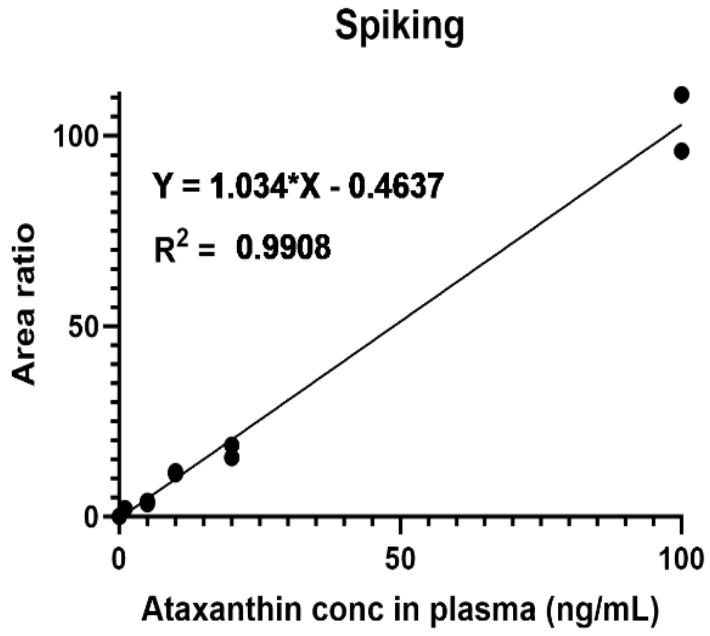

Figure 1. Calibration curve of ATX levles in the plasma was generated by spiking naive plasmas of n=2 untreated C57Bl/6 mice with the indicated concentrations of free ATX powder.

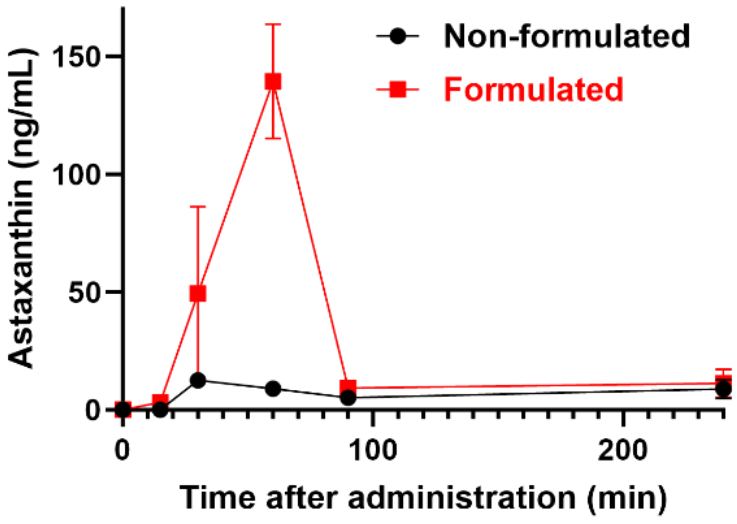

Figure 2. A pharmacokinetic profile (means ± SEM) of ATX in plasma of n=3/(time point) 4-week-old C57Bl/6 male mice treated with formulated (LDS-AXT) and non-formulated (AXT) astaxanthin as

 doi:10.20944/preprints202404.0556.v1

indicated. Area Under the Curve (AUC) values are 1597 ± 622 (95% Confidence Interval (CI): 377.9 to 2816) and 7012 ± 1882 (CI: 3323 to 10700) for ATX and LDS-ATX respectively.

2.2. *Antioxidant Efficacy of LDS-ATX v ATX*

The antioxidant capacity of ATX in comparison to LDS-ATX was tested in a pro-oxidant inducible system. To that end, mice were orally pretreated with ATX in oleoresin, or as LDS-ATX, for 24 h. Subsequently, oxidative stress was induced with 1 mg/kg LPS for 4 h and then the extent of pro-oxidant protection in brain, liver and muscle was determined using protein carbonylation and malondialdehyde commercial kits for respectively determining irreversible protein oxidation and lipid peroxidation oxidative damage. Wild type mice, not induced with LPS, were used to assess basal, non-induced, oxidative stress. We predicted that this oxidative stress will be significantly lower than the LPS-induced stress and therefore, based on its significantly improved pharmacokinetic profile, tested only the effect of LDS-ATX in non-LPS-induced mice. Our results show that indeed LPS induction produced a more than two-fold increase in both lipid peroxidation and protein oxidation in all organ tested. LDS-ATX did not affect this basal oxidative stress. Lipid peroxidation (Figure 3), presumably directly affected by the lipid soluble ATX, which is dissolved in cell membranes, was in general more affected by both ATX and LDS-ATX than protein oxidation (Figure 4). The most affected organ was the liver, which is also the most metabolically active organ. In the liver, both lipid peroxidation and protein oxidation were better ameliorated by LDS-ATX than by ATX. In the brain, lipid peroxidation was more attenuated by LDS-ATX than by ATX, but protein oxidation was attenuated to the same extent by both ATX formulations and to a lesser extent than lipid peroxidation. In the muscle, both lipid peroxidation and protein oxidation were significantly reduced only by LDS-ATX and not by ATX.

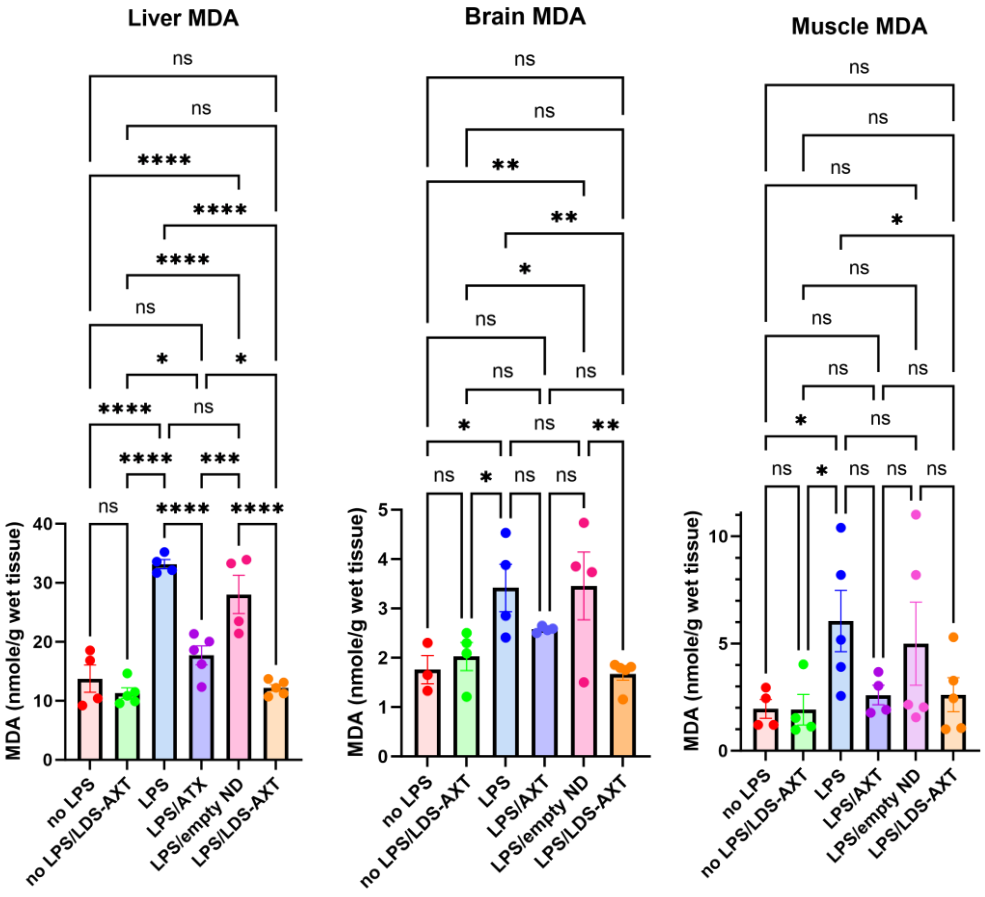

Figure 3. Malondialdehyde (MDA) levels in different tissues induced or not with LPS. MDA was determined by AbCam's ab233471 commercial kit, as a measure of lipid peroxidation in liver, brain, and gastrocnemius muscle homogenates collected from 8-month-old C57Bl mice. The results (outliers

 doi:10.20944/preprints202404.0556.v1

removed) show that LPS induced lipid peroxidation, which was attenuated by ATX and even more so by LDS-ATX. Basal, non-induced lipid peroxidation was not significantly affected by LDS-ATX. *, p<0.05; **, p<0.01; ***, p<0.001; ****, p<0.0001; ns = not significant. One-Way ANOVA with Fisher's post-hoc test.

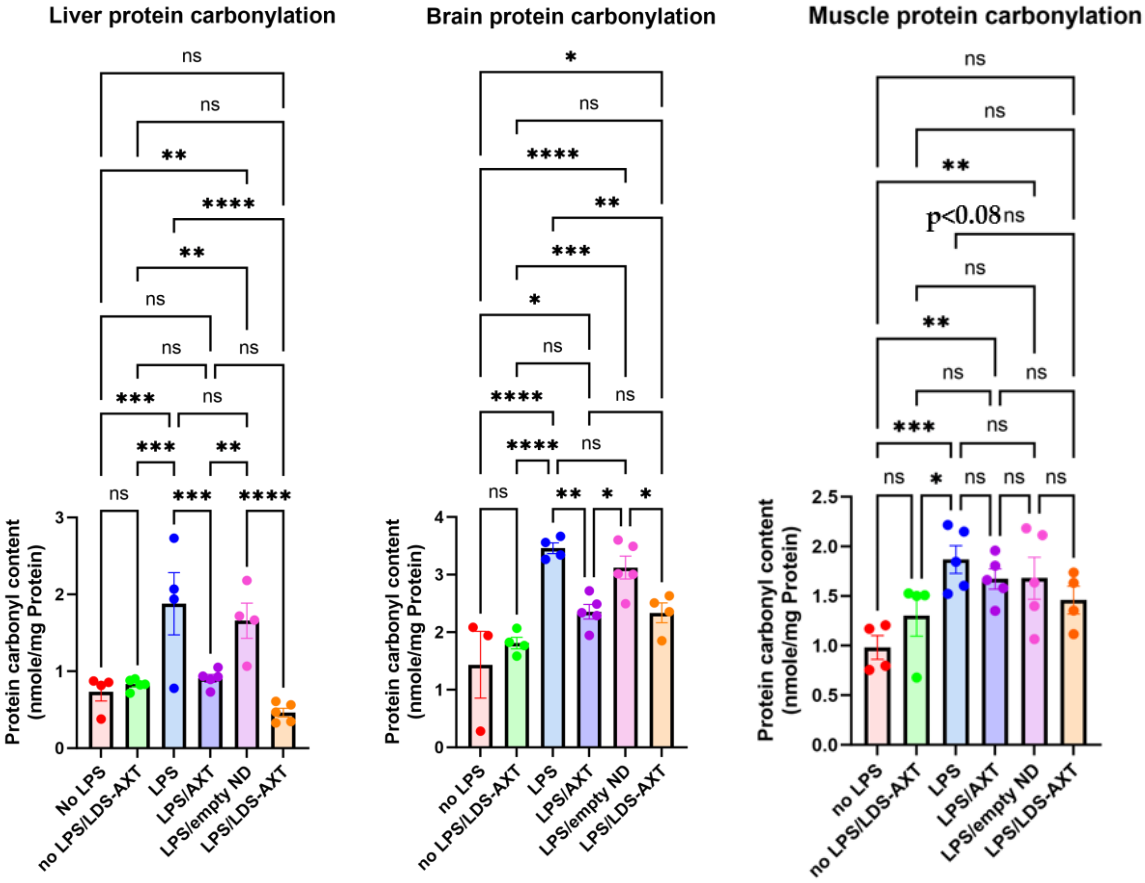

Figure 4. Protein carbonylation levels in different tissues induced or not with LPS. Protein carbonylation by 2,4-dinitrophenylhydrazine was determined by AbCam's ab126287 commercial kit, as a measure of protein irreversible oxidative damage in liver, brain, and gastrocnemius muscle homogenates collected from 8-month-old C57Bl mice. The results (outliers removed) show that LPS-induced protein oxidation, which was attenuated by ATX, was significantly further attenuated by LDS-AXT in the liver, attenuated to the same extent by ATX and LDS-ATX in the brain and attenuated only by LDS-AXT (p<0.08) and not by AXT in the muscle. Basal, non-induced lipid peroxidation was not significantly affected by LDS-ATX. *, p<0.05; **, p<0.01; ***, p<0.001; ****, p<0.0001. ns = not significant. One-Way ANOVA with Fisher's post-hoc test.

3. Discussion

Our unique LDS-ATX formulation, as all other LDS nanodroplet formulations, is a complex blend of co-solvents, hydrophilic, and hydrophobic surfactants, proportioned in a ratio meticulously studied and optimized during the development process. This unique combination results in a substantially hydrophilic delivery system. Importantly, this system is capable of maintaining the desired structural arrangement in a water-less state, and also facilitates the in-situ formation of these structures upon post-dilution in the gastrointestinal (GI) tract and stomach following oral administration. Here we tried to solubilize ATX by a tailored LDS nanodroplet. Several studies, using different types of formulations, have demonstrated a formulation-dependent improvement of stability and anti-oxidant capacity of ATX (*e.g.*, [2,6–8]). However, while many of these studies focus on cell-based assays for assessing the anti-oxidant capacity of the formulated ATX, few studies compare in parallel the anti-oxidant efficacy of formulated ATX in different organs and in basal and

 doi:10.20944/preprints202404.0556.v1

induced pro-oxidant conditions, while assessing oxidative damage to both lipids and proteins. In that respect, the comprehensive analysis of our study might better recapitulate physiological conditions and thus better predict the efficacy of LDS-ATX in humans.

The choice of protein carbonylation and lipid peroxidation as indicators of oxidative injury is not only comprehensive, but also more accurate: Protein carbonylation is a non-enzymatic irreversible post-translational modification of proteins induced by oxidative stress. Total protein carbonylation is considered an informative and reliable biomarker of oxidative stress since it reports irreparable oxidative damage to proteins, as opposed to other oxidative stress markers reporting production of reactive oxygen species, which could cause oxidative damage, but can also be repaired by the cells anti-oxidant machinery. Protein carbonyls are generated by oxidation of amino acid side chains into aldehydes and ketones and are quantified by derivatizing them with dinitrophenylhydrazone (DNPH) followed by DNPH immunodetection using enzyme linked immunosorbent assay (ELISA). The lipid peroxidation assay detects oxidation of mainly cell membrane-associated polyunsaturated fatty acids, which are ultimately peroxidized to malondialdehyde (MDA), detectable by its reaction with thiobarbituric acid reactive substances (TBARS) generating a spectrophotometrically quantifiable product which absorbs light at 532 nm.

Lastly, differences among the different organs in oxidative injury and its repair by LDS-ATX might results from various reasons and more in depth physiological and ex vivo investigation might be required to elucidate these differences. However, some suggestions can be presented here: Firstly, perfusion of the different organs is different, the liver being the most perfused organ and muscle probably the less perfused. These differences in perfusion probably explain why, in general, muscle was less influenced by both ATX and LDS-ATX compared to liver, and to a lesser extent compared to brain. Another difference among the different organs tested is in the relative membrane protein contents. This difference might account for the fact that while in the liver ATX and LDS-ATX reduced both protein and membrane oxidation, in the brain protein oxidation was influenced less than membrane oxidation. If the relative abundance of membrane associated proteins, such as transporters or channels, is higher in the liver than in the brain, we can conjecture that MDA peroxidation will affect juxtaposing proteins more in the liver than in the brain.

4. Materials and Methods

4.1. Preparation of Tailored Nano-Droplets for Astaxanthin Delivery (LDS-ATX)

Our oil-in-water confidential nano-formulation for ATX is based on a set of food-grade quality excipients permitted for oral use as food supplements. This tailored nano-formulation was developed by LDS to solubilize ATX. The maximum loading capacity was 1.0 wt%. This careful selection of ingredients underscores the commitment to ensure the highest standard of safety and quality in the development process.

The preparation of LDS-ATX involves a two-step process. Initially, empty concentrates were prepared by accurately weighing all the excipients and mixing them together with the aid of magnetic stirring plates. The concentrates were mixed while heated, using a water bath maintained at no more than 60°C. Once the solution achieved homogeneity (clear, transparent concentrate), the active compound, ATX in oleoresin (10 wt%), was introduced under nitrogen at a specified concentration, as presented in Figure 5. Subsequently, samples were mixed under heat, and maintained at 50 ± 10°C, until ATX (the active pharmaceutical ingredient, API) became fully solubilized in the concentrate. Since the formulation exhibits a dim color after adding the API, light microscope was used to confirm complete solubility.

 doi:10.20944/preprints202404.0556.v1

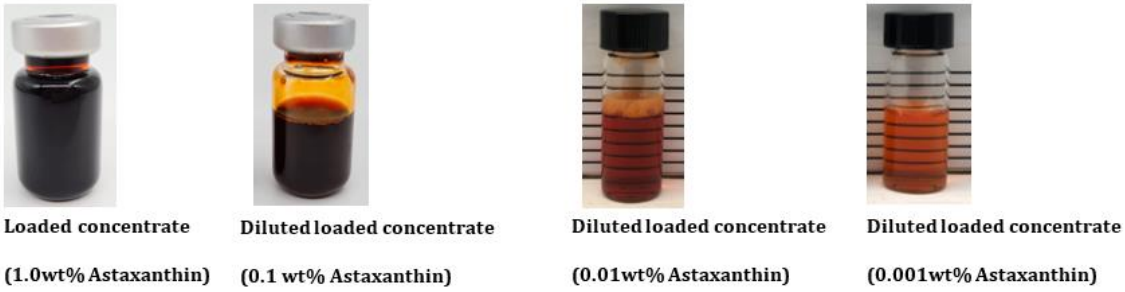

Figure 5. Visual appearance of the formulated loaded concentrate and its dilutions in water.

Nanodroplets size (Figure 6) was measured by dynamic light scattering using the Nano-S system (Malvern-Panalytical) equipped with a 633 nm laser, at 173° (back scattering). The operation was conducted using the Zetsizer® program. The sample underwent a significant dilution process (100 mg formulation diluted in 100 mL of purified water) prior to measurement. The transparency enabled by the dilution is crucial for the effective transmission of laser light passing through the sample without being obstructed by its density or opacity during analysis.

			Size (d.nm):	% Volume:	St Dev (d.nm):
Z-Average (d.nm):	27.21	Peak 1:	11.99	99.6	4.338
PdI:	0.601	Peak 2:	99.92	0.4	57.81
Intercept:	0.673	Peak 3:	0.000	0.0	0.000
Result quality :	Good				

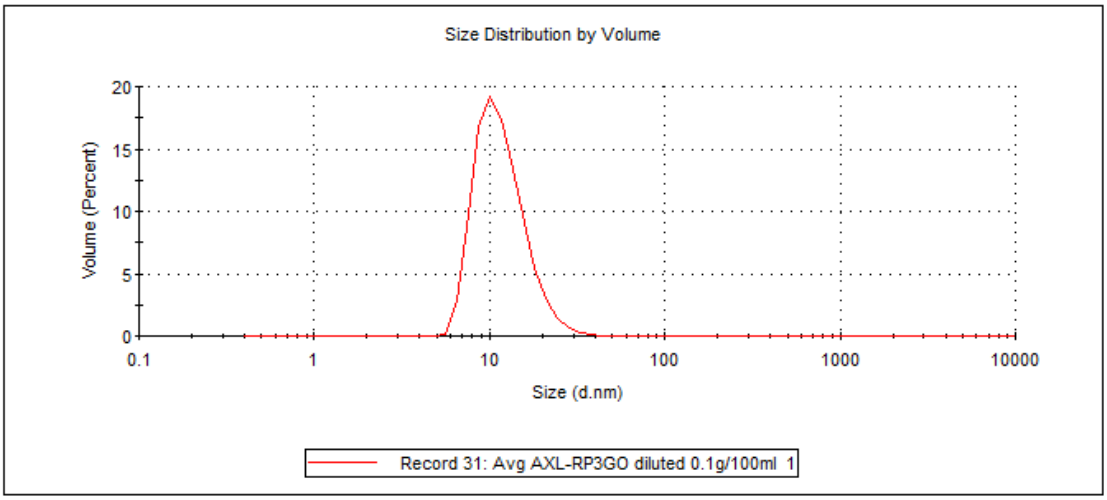

Figure 6. LDS-ATX droplet size determined by dynamic light scattering (DLS). Average droplet size is 11.99 nm with only very minor populations of higher sized droplets.

LDS-ATX physical stability (Figure 7) was measured using the LUMiSizer® dispersion analyzer (LUM, GmbH, Berlin, Germany) in 2 mm polycarbonate cuvettes shined at 856 nm at 25°C. The LUMiSizer® monitors light transmission through the samples while they are centrifuged horizontally. The change in transmission indicates the stability of the systems because when the transmission profiles remain constant, the samples are considered physically stable. The samples shelf-life can be extrapolated based on the measurement conditions using the following formula:

$$Shelf\ life = rcf \times (number\ of\ profiles) \times interval$$

In our case, transmission did not degrade even after 800 profiles (cycles) were run at 1,000 rcf with 60 sec intervals between measurements and therefore the extrapolated physical shelf-life of LDS-ATX is approximately 2 years.

 doi:10.20944/preprints202404.0556.v1

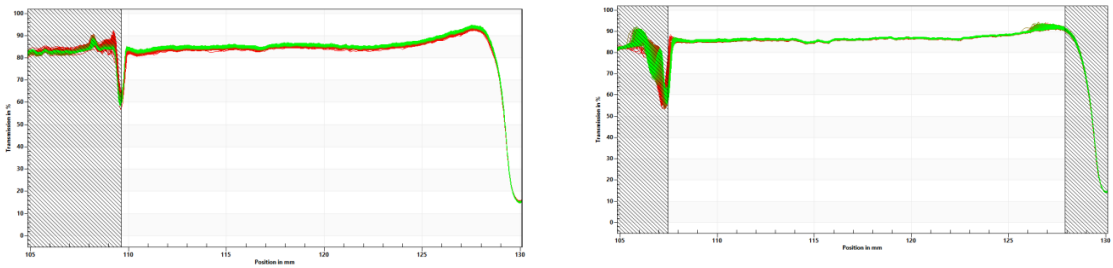

(**A**) (**B**)

Figure 7. Physical stability measured by LUMiSizer® for **(A)** concentrated system (1.0wt% Astaxanthin) and **(B)** diluted system (0.1% Astaxanthin). Transmission profiles (Y axis) were plotted as a function of position (X axis) and time (line color). No significant changes in transmission were observed in both concentrated and diluted systems, meaning that the systems are physically stable.

4.2. Liquid Chromatography Tandem Mass Spectrometry (LC-MS/MS)

4.2.1. LC-MS/MS Materials

LC/MS-grade Acetonitrile (ACN), Methanol and water were purchased from Biolab Ltd. (Jerusalem, Israel). LC/MS-grade Formic acid (FA) was purchased from Fisher Chemical™ Optima™ (USA). Apo-8-carotenal (APO), used as internal standard (IS), was purchased from Merck.

4.2.2. Ultra-High Performance Liquid Chromatography (UHPLC)

LC-MS/MS analyses were conducted on a Sciex (Framingham, MA, USA) Triple Quad™ 5500 mass spectrometer coupled with a Shimadzu (Kyoto, Japan) UHPLC System. The chromatographic separations were performed on a CORTECS® (Waters Corp., Milford, MA, USA) column (C18, 2.7 µm particle size, 50 x 2.1 mm), protected by a VanGuard® (Waters Corp., Milford, MA, USA) cartridge (CORTECS® C18, 5 x 2.1 mm). The injection volume was 5 µL. The oven temperature was maintained at 40°C and the autosampler tray temperature was maintained at 10°C.

The chromatographic separation was achieved using a linear gradient program at a constant flow rate of 0.4 mL/min over a total run time of 7 min. An outline of the mobile phase gradient program is summarized in Table 1.

Table 1. Gradient program: Solvent A is 0.1% formic acid (FA) in water and solvent B is 0.1% FA in ACN.

Time (min)	Solvent A (%)	Solvent B (%)
0.0	23	77
0.5	23	77
2.5	5	95
4.5	5	95
5.0	23	77
7.0	23	77

The column effluent was diverted away from the MS during the first 0.7 min and the last min of the run. Methanol was used for washing the needle prior to each injection cycle. All samples were analyzed in duplicate.

4.2.3. MS/MS Conditions

ATX and APO (IS) were detected in positive ion mode using electron spray ionization (ESI) and multiple reaction monitoring (MRM) mode of acquisition.

 doi:10.20944/preprints202404.0556.v1

The molecular ions of the compounds [M+H]+ were selected in the first mass analyzer and fragmented in the collision cell followed by detection of the products of fragmentation in the second analyzer. Their transitions are shown in Table 2.

Table 2. Multiple reaction monitoring (MRM) transitions and parameters for ATX and APO (IS) in positive ion mode. m/z: mass to charge ratio; DP, declustering potential; CE, collision energy; CXP, collision cell exit potential; V, volts; eV, electronvolts; Rt, retention time.

Name	Precursor (m/z)	Product (m/z)	DP (V)	CE (eV)	CXP (V)	Rt (min)
ATX	597.3	Quantifier 147.2	6	29	16	2.0
		Qualifier 173.1	11	23	10	
APO	417.2	Quantifier 325.2	16	13	12	3.8
		Qualifier 159.2	21	27	16	

The TurboIonspray® probe temperature was set at 600°C with the ion spray voltage at 5500 V. The curtain gas was set at 25.0 psi. The nebulizer gas (Gas 1) was set to 50 psi, the turbo heater gas (Gas 2) was set to 10 psi and the collision gas (CAD) was set to 8 psi. The entrance potential (EP) was set at 10 V. The collision energy potentials (CE), collision cell exit potentials (CXP) and declustering potentials (DP) for the monitored transitions are given in Table 2. The dwell time was 20 ms. Data acquisition and analysis were performed using Analyst 1.6.3 software distributed by Sciex. Quantitative calibrations (0–100 ng/mL) of ATX were performed before every batch of samples using peak-area ratios (compound versus internal standard). The calibration curve (y = a + bx) was obtained by weighted (1/y) linear least-squares regression of the measured peak-area ratio (y) versus the concentration added to the plasma (x). The limit of quantification (LOQ) was 1 ng/mL for ATX. A typical chromatogram of ATX in plasma is shown in Figure 8.

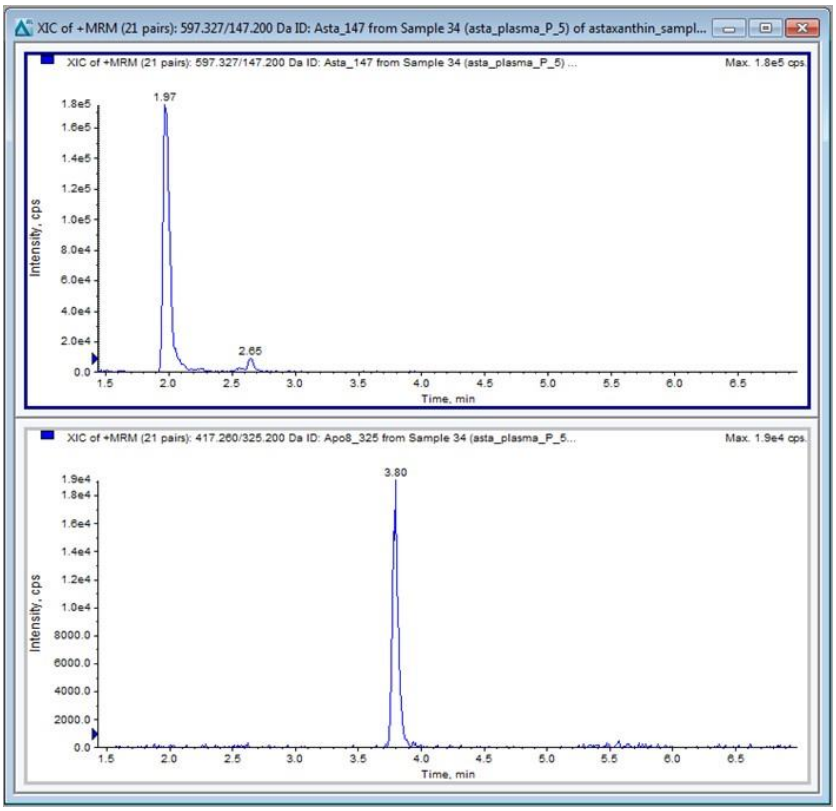

Figure 8. A typical chromatogram of ATX (upper panel), and the APO IS (lower panel) in a mouse plasma sample.

 doi:10.20944/preprints202404.0556.v1

4.3. Pharmacokinetics

To determine the distribution and kinetic parameters of ATX in blood, 4-week-old C57Bl/6 male mice were pipetted *per os* 10 mg/kg ATX either as a non-formulated compound dispersed in oleoresin solution, as control, or as the tested LDS-ATX. Mice (n=3/time point) were euthanized by cervical dislocation 0, 15, 30, 60, 90, and 240 min post administration. Blood was then collected by cardiac puncture and extracted with 1:1 acetonitrile following established guidelines. The level of ATX in plasma was analyzed by LC-MS/MS as described above.

4.4. In Vivo and Ex Vivo Studies

The antioxidant effect of ATX and LDS-ATX was tested using a lipopolysaccharide (LPS)-inducible system. LPS is a Gram-negative bacterial endotoxin which acts as a strong stimulator of innate immunity generating pro-inflammatory oxidative stress. We pretreated 8-month-old C57Bl mice *per os* with 10 mg/kg ATX or LDS-ATX for 24 h, and then induced oxidative stress with 1 mg/kg LPS for 4 h. We subsequently extracted brain, liver and muscle tissues from the mice and quantified in them the extent of pro-oxidant protection using protein carbonylation ELISA kit (Abcam, AB-ab238536-96) and lipid peroxidation (malondialdehyde) kit (Abcam, AB-ab118970-100), all (*i.e.*, extraction and quantification) as per the manufacturer instructions. Mice not induced with LPS were used to assess the basal non-induced oxidative stress and whether such stress can also be corrected by ATX. The experimental layout is shown in Table 3.

Table 3. Experimental layout for the animal study.

LDS-ATX	ATX	Unloaded nanodroplet	LPS	# of animals
+	-	-	+	5
-	-	+	+	5
-	+	-	+	5
-	-	-	+	5
+	-	-	-	5
-	-	-	-	5

4.5. Statistical Analysis

All statistical analyses were performed by Prism GraphPad v. 10. $p<0.05$ was used as the significance value for rejecting null hypotheses. One Way ANOVA with Fischer post-hoc LSD tests were used for multiple comparisons (Figures 3 and 4).

5. Conclusions

In conclusion, our tailored ATX nano-formulation LDS-ATX can significantly improve the biodistribution of ATX. Lipid peroxidation is further attenuated by LDS-ATX, as compared to ATX, in liver, muscle and brain, while protein oxidation is more attenuated by LDS-ATX, as compared to ATX, only in liver and muscle.

Author Contributions: Conceptualization, O.K. and N.G.; Methodology, K.M., N.K., D.B.; Writing—original draft preparation, O.K.; writing—review and editing, O.K., N.K., D.B., S.G., N.G.; supervision, O.K., N.G.; Funding acquisition, N.G. and S.G. All authors have read and agreed to the published version of the manuscript.

Funding: Please add: This research was funded by Lyotropic Delivery Systems (LDS) Ltd.

Institutional Review Board Statement: The animal study protocol was approved by the Institutional Animal Care and Use Committee of The Hebrew University of Jerusalem (protocol code 17269 approved on 20 Feb 2024).

Conflicts of Interest: N.K., S.G. and N.G. are employed by the company LDS which designed and manufactured LDS-ATX.

 doi:10.20944/preprints202404.0556.v1

References

1. Y. Nishida, E. Yamashita, and W. Miki, "Quenching Activities of Common Hydrophilic and Lipophilic Antioxidants against Singlet Oxygen Using Chemiluminescence Detection System " *Carotenoid Science,* vol. 11, pp. 16-20, 2007.
2. B. Eren, S. Tuncay Tanrıverdi, F. Aydın Köse, and Ö. Özer, "Antioxidant properties evaluation of topical astaxanthin formulations as anti-aging products," (in eng), *J Cosmet Dermatol,* vol. 18, no. 1, pp. 242-250, Feb 2019, doi: 10.1111/jocd.12665.
3. D. Madhavi, D. Kagan, and S. Seshadri, "A Study on the Bioavailability of a Proprietary, Sustained-release Formulation of Astaxanthin," (in eng), *Integr Med (Encinitas),* vol. 17, no. 3, pp. 38-42, Jun 2018.
4. N. Garti, "Delivery of microparticulated liquid systems in food," vol. 3, (Handb. Nonmed. Appl. Liposomes: CRC Press, 2018, pp. 143-198.
5. Y. Prigat, A. Fattori, A. I. Shames, M. F. Ottaviani, and N. Garti, "Micro-characterization of modified microemulsions loaded with gossypol, pure and extracted from cottonseed," (in eng), *Colloids Surf B Biointerfaces,* vol. 180, pp. 487-494, Aug 01 2019, doi: 10.1016/j.colsurfb.2019.05.004.
6. E. J. Hwang, Y. I. Jeong, K. J. Lee, Y. B. Yu, S. H. Ohk, and S. Y. Lee, "Anticancer Activity of Astaxanthin-Incorporated Chitosan Nanoparticles," (in eng), *Molecules,* vol. 29, no. 2, Jan 21 2024, doi: 10.3390/molecules29020529.
7. Y. Liao *et al.*, "Preparation of astaxanthin-loaded composite micelles with coaxial electrospray technology for enhanced oral bioavailability and improved antioxidation capability," (in eng), *J Sci Food Agric,* vol. 104, no. 3, pp. 1408-1419, Feb 2024, doi: 10.1002/jsfa.13019.
8. F. Yu *et al.*, "Preparation of carrier-free astaxanthin nanoparticles with improved antioxidant capacity," (in eng), *Front Nutr,* vol. 9, p. 1022323, 2022, doi: 10.3389/fnut.2022.1022323.